Astron. Astrophys. 325, 1088–1098 (1997)

ASTRONOMY AND ASTROPHYSICS

Aluminium in metal-poor stars⋆

D. Baumüller and T. Gehren

Institut für Astronomie und Astrophysik der Universität München, Scheinerstr. 1, D-81679 München, Germany (gehren@usm.uni-muenchen.de)

Received 19 November 1996 / Accepted 10 April 1997

Abstract. Previous calculations of the statistical equilibrium of aluminium in the solar photosphere have shown that NLTE populations hardly affect Al *line formation* in the Sun; however, in metal-poor stars the influence of electron collisions is reduced, and a UV radiation field enhanced due to smaller background line opacity results in more pronounced NLTE effects. Thus analyses based on NLTE populations lead to significantly higher Al abundances than those calculated from LTE. For stars of intermediate metallicity between $-1.0 <$ [Fe/H] < -0.5 some overabundance relative to iron is found. For more metal-poor stars the overabundance disappears and approaches the solar ratio, [Al/Fe] = 0. Only a weak overabundance in the [Al/Mg] ratio is detected for stars with intermediate metallicity and a small underabundance of -0.2 to -0.3 dex for the metal-poor stars. From investigation of both solar and stellar Al spectra the influence of *hydrogen collisions* could be better estimated. The previously defined atomic model thus had to be slightly modified to fit both metal-rich and metal-poor stars.

Compared with LTE analyses the present results completely change the chemical enrichment scenario with [Al/Fe] now following the trend of *primary* elements for all metal-poor stars. The hump of enhanced Al/Fe values for stars between $-1.0 <$ [Fe/H] < -0.5 does *not* seem to be an artefact. It nearly vanishes for the [Mg/Fe] abundance ratios. It may not necessarily have to be explained in terms of stellar nucleosynthesis because it could result from our reference to LTE abundances for Mg and Fe.

Key words: atomic processes – nucleosynthesis – lines: formation – stars: abundances – Galaxy: abundances

1. Introduction

Due to the extra neutron in its nucleus aluminium is of special concern whenever the nucleosynthesis of light elements during the first stages of Galaxy formation is under investigation. Similar to sodium which will be discussed in a separate paper and phosphor which cannot easily be analyzed in sufficiently metal-poor stars, the synthesis of ^{27}Al requires either an explosive event that provides neutrons on a very short time scale or the production or pre-existence of neutrons in that part of a star that undergoes *stationary* burning processes. Knowing the variation of the neutron-enriched light elements with respect to α-elements such as Ne, Mg or S as a function of Galactic chemical enrichment may in fact lead to a better understanding of what processes have dominated the very early stages of Galactic evolution. Today it is generally accepted that α-nuclei such as ^{24}Mg are predominantly synthesized during Supernova explosions of type II (e.g. Nomoto et al. 1984; Woosley et al. 1986; Thielemann et al. 1986). It is therefore not surprising that the [Mg/Fe] ratio is above solar for halo stars (Fuhrmann et al. 1995), since Fe itself is mostly added to the interstellar medium in later stages of Galactic evolution as a result of Supernovae of type Ia. The formation of ^{23}Na and ^{27}Al may be more complex since a reservoir of neutrons must become available during their synthesis.

Recently, Woosley & Weaver (1995) have published an updated list of nuclear processes that are expected in SN II. According to their calculations ^{23}Na must be synthesized mostly during *hydrostatic* carbon burning through ^{12}C (^{12}C,p) ^{23}Na , with a small admixture from both the ^{22}Ne (p,γ) ^{23}Na reaction during hydrostatic H shell burning, and the neutron capture of ^{22}Ne during He shell burning processes. Hydrostatic carbon burning allows the neutron excess to gradually increase and thus the reaction products do not depend much on chemical evolution. The shell burning processes, however, require the preexistence of a neutron source such as ^{22}Ne. ^{27}Al is synthesized similarly during *hydrostatic* carbon and neon burning, whereas ^{24}Mg is produced in both hydrostatic and explosive neon burning. Nomoto et al. (1984) have predicted that SN Ia synthesize ^{23}Na or ^{27}Al nuclei only 10^{-3} to 10^{-4} times as abundant than ^{24}Mg and therefore are completely unimportant for the production of these neutron-rich nuclei. Such a scenario would predict a slightly *different* chemical evolution for ^{23}Na and ^{27}Al , in particular it predicts a predominantly *primary* origin for ^{27}Al with [Al/Mg] ≈ 0 throughout the early stages of Galactic evolution.

Timmes et al. (1995) used these predictions to compare [Al/Fe] and [Al/Mg] abundance ratios with the results obtained

Send offprint requests to: T. Gehren

⋆ Based on observations collected at the European Southern Observatory, La Silla, Chile, and at the German-Spanish Astronomical Center, Calar Alto, Spain

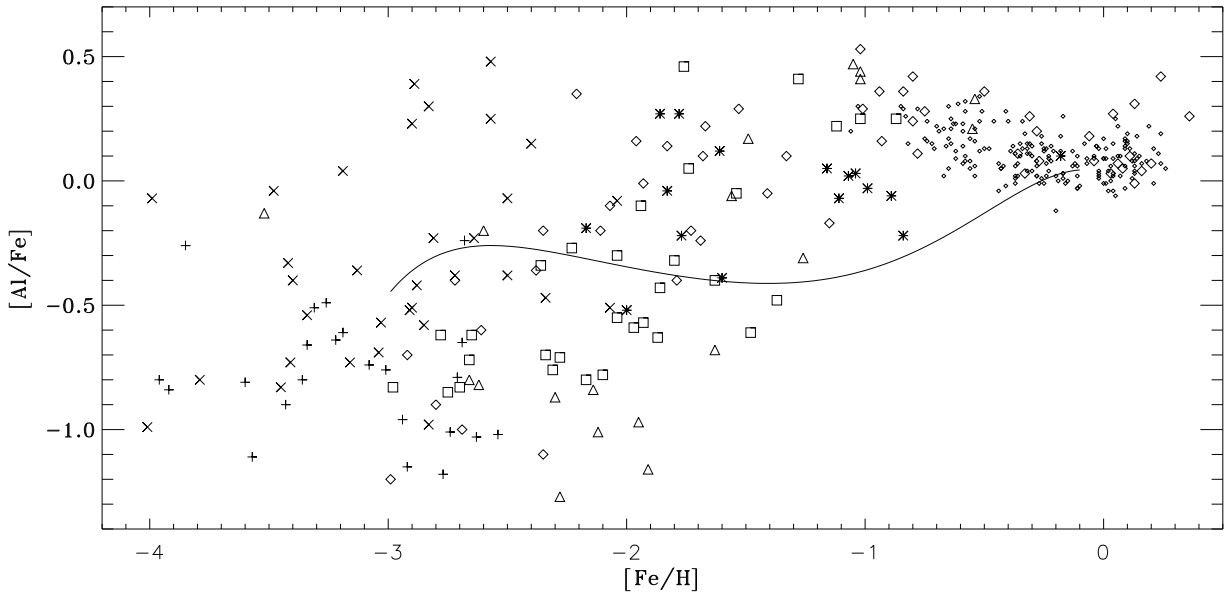

Fig. 1. Aluminium abundances of metal-poor stars determined from LTE analyses of Peterson (1981, △), Gratton & Sneden (1987, 1988, ◇), Magain (1987, 1989, □), Hartmann & Gehren (1988, ∗), Edvardsson et al. (1993, small diamonds), McWilliam et al. (1995, ×), and Ryan et al. (1997, +). The curve represents the standard chemical evolution model calculated by Timmes et al. (1995).

from the quantitative spectrum analyses of metal-poor stars. The abundance pattern of aluminium in such cool metal-poor stars has emerged from LTE analyses (Peterson 1981; Magain 1987, 1989; Hartmann & Gehren 1988; Gratton & Sneden 1988; Edvardsson et al. 1993; McWilliam et al. 1995; Ryan et al. 1997), and it shows a significant underabundance of alumimium compared to either iron or magnesium for most stars with [Fe/H] < -1. At intermediate metal abundances, $-1 <$ [Fe/H] the [Al/Fe] and [Al/Mg] ratios are found to be essentially solar, with only marginally different trends. Gratton & Sneden (1987) and McWilliam et al. (1995) detected some overabundance of [Al/Fe] in a number of extremely metal-poor objects. The scatter is large, and particularly the transition from solar values to lower metallicity is badly defined in both position and shape. Whenever different multiplets were analyzed some discrepancy appeared between the abundances derived from these lines. This is seen in Fig. 1; Edvardsson et al. investigated the lines around 8773 Å, Peterson, McWilliam et al. and Hartmann & Gehren used both resonance lines, Magain, and Gratton & Sneden the resonance line at 3961 Å.

The inconsistencies of abundances obtained from different Al lines are partly hidden in the overall scatter of the data in Fig. 1. Both could be the result of either

- systematic *temperature* errors due to different methods of temperature determination,
- problems with the detection of the continuum in the region around the resonance lines. This is a general problem since the resonance lines both reside on the strong line wings of Ca II H and K. Furthermore the background opacity due to metallic lines is strong in this wavelength region, and it results in an additional depression of the continuum,
- the invalidity of the LTE assumption,

or a combination of the above. In less metal-poor stars the red lines at 8773 Å and the weaker ones at 6696 Å may be easier to analyze, however, it is necessary to bear in mind that in stars with [Fe/H] < -1 these lines are too weak to be observed with high enough accuracy. There the resonance lines are the only source of reliable aluminium abundances. As is obvious from the solar spectrum the resonance line at 3944 Å is blended. Arpigny & Magain (1983) pointed out that the blend is due to CH. While temperature errors cannot be ruled out as a source of discrepancies we note that the resonance lines are strongly affected by ground state ionization, and therefore NLTE effects could explain why observed aluminium abundance ratios and those predicted from chemical evolution differ so significantly in Fig. 1.

Such NLTE calculations have been carried out for aluminium in metal-poor stars. A previous investigation (Baumüller & Gehren 1996, Paper I) has demonstrated how the line profiles found in the solar spectrum are used to improve the atomic model of Al I. This model is the subject of further scrutiny in the light of information coming from test calculations and observational evidence found in the spectra of metal-poor stars. Thus the current approach is an iterative one. We start with test calculations using the standard model atom of Paper I and standard atmospheric models as described in the next section. Section 3 deals with the amount of collisions by neutral hydrogen atoms necessary to establish a consistent atomic model for stars of *all* degrees of metal abundance by introduction of a *scaling factor* $S_{\rm H}$. Fortunately, this iteration with some observed spectra is successful, and in Sect. 4 the Al abundances in metal-poor stars are calculated from observed spectra based

on either LTE or NLTE level populations. The differences are significant, and they are therefore discussed in the final section.

2. NLTE line formation

The goal of this analysis is a differential one that employs techniques to specify *relative* abundances with respect to their solar values. It is therefore necessary to use a common model for both the aluminium atom and the atmospheric structure. The atmospheric models have been in use now for many years (Gehren 1977). They include full statistical line blanketing using the recent opacity distribution functions (ODF) made available by Kurucz (1992), convection according to the mixing-length approach quantified by Vitense (1953) and Böhm-Vitense (1958), where our choice of the mixing-length parameter is $\ell/H_p = 0.5$, as determined by Fuhrmann et al. (1993) from Balmer line fits. As mentioned it was found necessary to improve the atomic model while investigating the spectra of other metal-poor stars. Thus the atomic model only *starts* with the standard model used for the *solar* NLTE analysis. As in Paper I all line formation calculations are done with the DETAIL code (see Butler & Giddings 1985).

2.1. The standard atomic model

The standard atomic model is basically the same as that used for the solar calculations (Paper I). It consists of 51 terms of the Al I doublet system, of which fine structure is resolved only for the ground state. The doublet terms are complete up to $n = 10$ and $L = n - 1$. Additionally, each term with principal quantum number n between 11 and 15 is grouped together to form artificial 'superterms' identified only by their n. The system is closed by $3s^2\,{}^1\mathrm{S}$, the groundstate of Al^+. The terms are coupled by radiative and collisional interactions as described in more detail in Paper I.

We note that this standard model is dominated by the groundstate photoionization edge near 2073 Å , by far the largest ionization cross-section among all important ions in solar-type stars. Even under strong thermalization due to electron and atom collisions as found in the solar photosphere, photoionization dominates and produces overionization and a corresponding underpopulation of the $3p\,{}^2\mathrm{P^o}$ ground state in atmospheric layers as deep as $\tau_c = 1$! To evaluate the possible effects in different stellar atmospheres it is necessary to recall the influence of radiative and collision processes of different kinds. Whereas the depopulation of the Al I ground state through photoionization is already extreme in the Sun (which is a main-sequence star with comparatively strong collisional interaction), it is expected to increase even more in all *metal-poor* stars. The reason for this trend is the strong decrease of line blanketing, a corresponding increase of the radiation field and thus the photoionization rate. Since the metals are the important electron donators in cool stellar atmospheres the electron collision rates in metal-poor stars will drop. Thus in stars more metal-poor than the Sun a reduced thermalization efficiency of electron collisions is predicted.

Imagine now that collisional interactions were mostly due to encounters with neutral hydrogen atoms. As we have shown in Paper I, this will *not* affect the results obtained for most of the solar Al I lines except those in the IR. However, since collisional interactions with neutral hydrogen are *not* varying with metal abundance, they can maintain an important influence in metal-poor stellar atmospheres and raise the total collision rates to high enough efficiency at which they can even compensate the strongly increased photoionization. While radiative interactions can be treated on the basis of quite accurate data, this is not the case for collisional interactions. In particular the rates for collisions with neutral hydrogen can only be calculated by very poor approximations. As outlined in Paper I the hydrogen collisions are represented by Drawin's (1968, 1969) formula using the more recent reformulation of Steenbock & Holweger (1984). A closer look reveals that it is based on a simple adaptation of van Regemorter's (1962) treatment of electron collisions, with an additional scaling factor S_H that can be adjusted to fit an observed spectrum.

It is therefore that the investigation of solar *and* stellar spectra can help to define a semi-empirical but more reliable atomic collision model. While the far IR photospheric emission lines of the solar spectrum definitely rule out strong collisional coupling among highly excited levels implying a *collision strength factor* $S_\mathrm{H} \ll 1$ at energies above 5 eV, this factor remains largely undetermined for the visible and red lines commonly used for abundance analyses. Spectra of metal-poor stars are then required to determine the S_H factor for the collisions between the lower levels. This is achieved by comparison of abundances derived from different lines in the visible/red wavelength regions. Section 3 will show that a scaling factor has to be used that depends on excitation energy.

To estimate the problems connected with electron and hydrogen collisions between levels of Al I, it is important to recognize their different influence on the level populations in the solar atmosphere. In principle one might think of replacing e.g. the hydrogen collisions by a corresponding increase of the electron collisions. This does not lead to a better fit of the profiles, probably because electron collisions are most important in the inner photosphere whereas hydrogen collisions take over to dominate the atmospheric depths around $\tau_c = 0.01$. From solar observations alone it is therefore almost certain that Al I line formation depends on hydrogen collisions.

2.2. Test calculations for different stellar parameters

As outlined in paper I the statistical equilibrium of the neutral aluminium atom is determined mainly by two types of processes. One is the depopulation of the ground state by photoionization and the other one is the 'photon suction' described by Bruls et al. (1992). The lower levels are populated by electrons cascading downwards via line transitions of high transition probability. In aluminium this is the case for transitions of the type $\Delta n = 0$ or 1. The solar atmosphere is optically thick in these strong lines at atmospheric depths where collisional interactions are of low efficiency. Thus the energy of the line photons

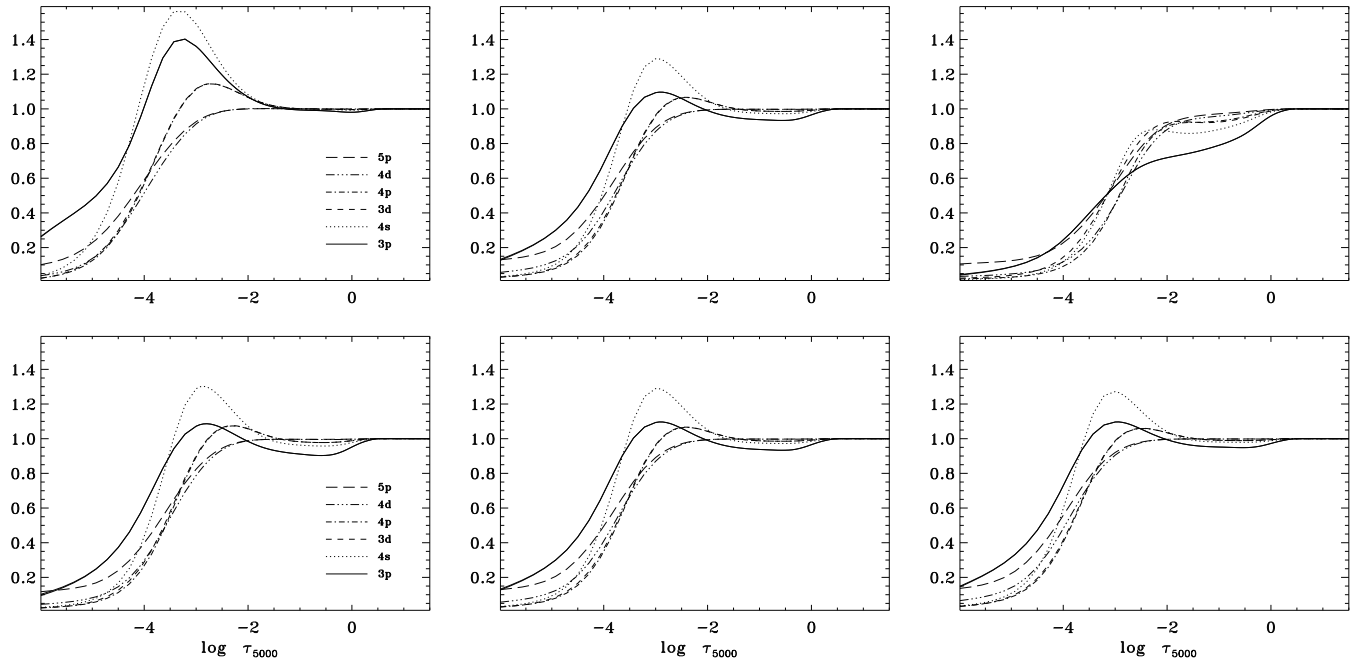

Fig. 2. Selected Al I level departure coefficients calculated in atmospheric models with different stellar parameters. Numbers refer to the usual definition, $b_i = n_i/n_i^{\rm LTE}$. *Top row from left to right*: Variation with temperature from 5300 to 5780 and 6000 K. *Bottom row from left to right*: Variation with gravity from $\log g$ = 4.00 to 4.44 and 4.70. Other parameters are kept at their solar value. The atomic model includes hydrogen collisions with a scaling factor $S_{\rm H}$ = 0.4

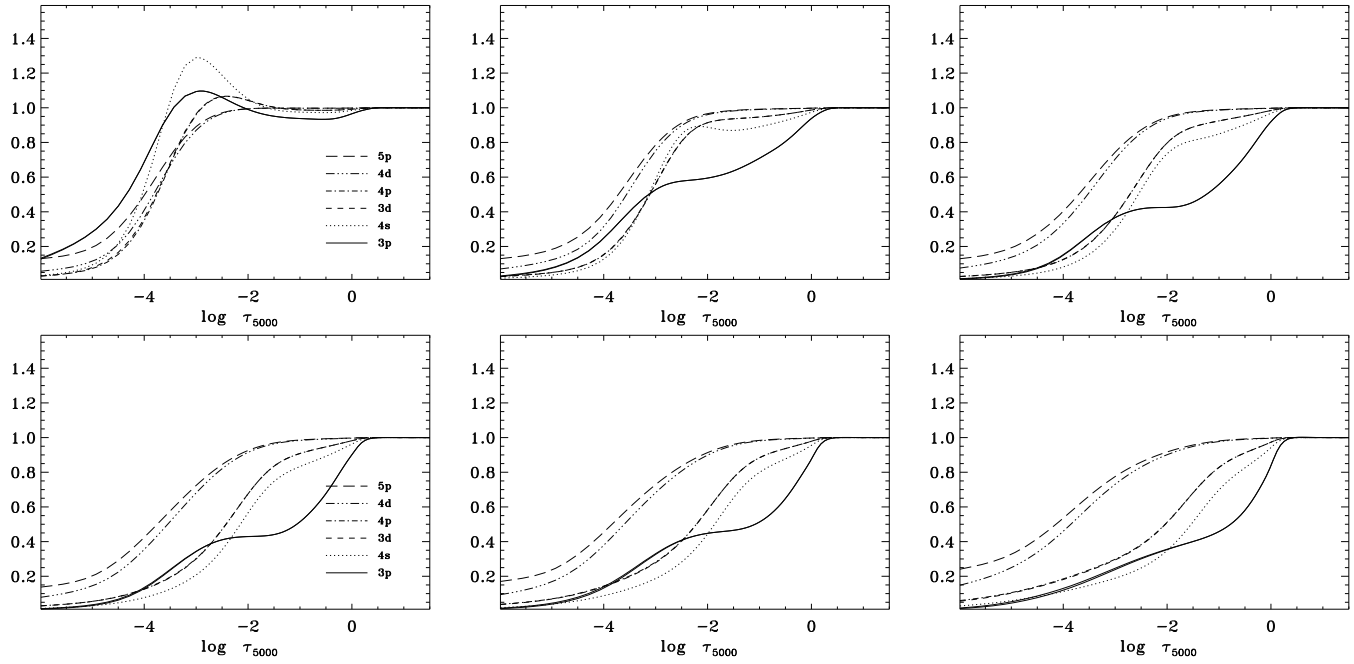

Fig. 3. Selected Al I level departure coefficients calculated in atmospheric models of *decreasing metallicity* with [Fe/H] = 0.0, –0.5, –1.0 in the top row and –1.5, –2.0 and –2.5 at the bottom (*from left to right*). $T_{\rm eff}$ and $\log g$ are kept at their solar value. The atomic model includes hydrogen collisions with a scaling factor $S_{\rm H}$ = 0.4. Note the small changes between [Fe/H] = –1.0 and –2.0

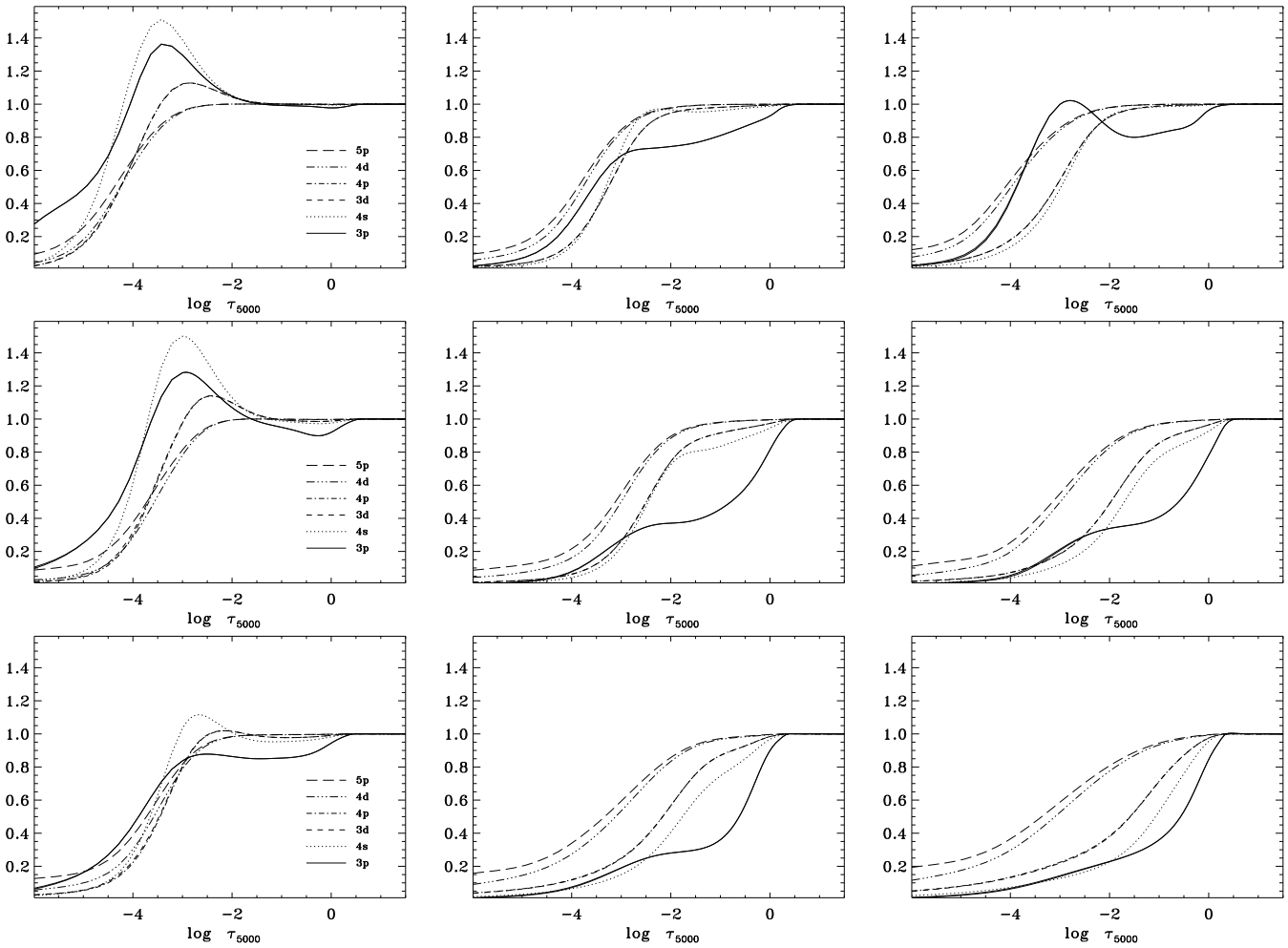

Fig. 4. Al I level departure coefficients for different model atmospheres. *Columns from left to right*: [Fe/H] 0.0, –1.0, and –2.0. *Top row*: $T_{\rm eff}$ = 5200 K, $\log g$ = 4.5 (cool subdwarf). *Middle row:* $T_{\rm eff}$ = 5500 K, $\log g$ = 3.5 (typical subgiant). *Bottom row:* $T_{\rm eff}$ = 6500 K, $\log g$ = 4.0 (Procyon-type turnoff star). The calculations include hydrogen collisions with a slightly different scaling factor $S_{\rm H}$ = 0.2

is not thermalized and they can be scattered over long distances. The resulting statistical equilibrium is reached with relatively overpopulated lower line levels. Both processes are visible in the departure coefficients of neutral aluminium. In the top left panel of Fig. 3 (the solar reference model) the ground state $3p\,^2{\rm P^o}$ is underpopulated inside $\log\tau_{\rm c} \approx -2$ which is a result of photoionization. Further outside around $\log\tau_{\rm c} = -2.5$ the photon suction results in an overpopulation of the lower levels.

In an atmosphere with reduced metal content the number density of free electrons is smaller, and the influence of radiative processes on the statistical equilibrium increases. Simultaneously, a lower background opacity in the UV will lead to an enhanced ground state ionization which can outweight the photon suction process in metal-poor stars. Non-solar temperatures and gravities also affect the statistical equilibrium. To isolate the single influences we start with a series of test calculations with the solar model as a reference, and only one of the basic stellar parameters $T_{\rm eff}$ and $\log g$ is changed at a time. The atomic model is similar to the *standard* model used for the Sun (cf. Paper I) where the hydrogen collisions are scaled by a factor of $S_{\rm H} = 10/27 \approx 0.4$.

It was mentioned above that in the Sun the aluminium ionization edge at 2073 Å is one of the most prominent features in the UV region. Therefore the statistical equilibrium of aluminium in the Sun is determined by the interaction of the ground state ionization rate and transitions via a few red and IR lines. A change in temperature will predominantly affect the radiation field and thus influence photoionization rates and the resulting statistical equilibrium. The departure coefficients as shown in the upper panels of Fig. 2 are obviously quite sensitive to even relatively small changes in temperature. This is easily understood since the UV radiation field near the ground state ionization edge is strongly varying; thus reduction of the temperature results in considerable weakening of the atmospheric mean UV intensities. It is also evident from the stronger thermalization in the lower photosphere where the ground state ionization has almost disappeared and the lower levels are overpopulated outside $\log\tau_{\rm c} = -2$. The cascading process via strong line transitions

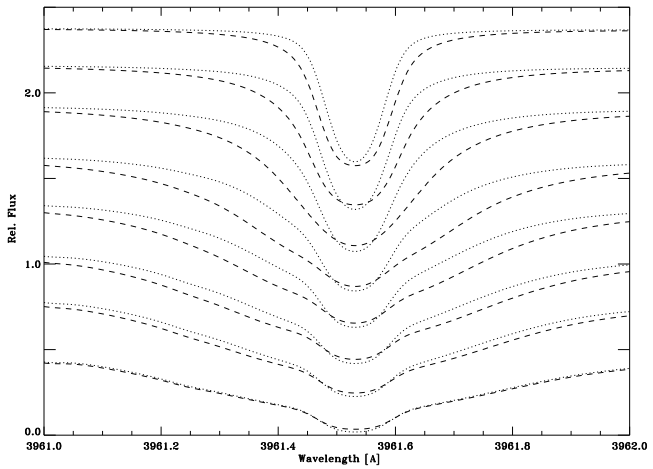

Fig. 5. Aluminium resonance line calculated from LTE (dashes) and NLTE (dots) line formation in atmospheres of different metal abundance; [Fe/H] (*from top to bottom*): –2.5, –2.0, –1.5, –1.0, –0.75, –0.5, –0.35, and 0.0. Profiles are shifted vertically by 0.2 flux units with respect to each other. They account for the opacity of the Ca II H and K and Hε line wings

Table 1. [Al/H] Abundance differences between NLTE and LTE line formation fitting the line equivalent width calculated under assumption of LTE

$T_{\rm eff}$	log g	[Fe/H]	Δ[Al/H]$_{\rm NLTE-LTE}$	
			3961 Å	6697 Å
5200	4.50	0.0	0.00	–0.01
5200	4.50	–1.0	0.18	0.04
5200	4.50	–2.0	0.12	
5200	4.50	–3.0	0.22	
5500	3.50	0.0	0.04	0.01
5500	3.50	–1.0	0.58	0.18
5500	3.50	–2.0	0.52	
5500	3.50	–3.0	0.65	
5780	4.44	–0.0	0.06	0.04
5780	4.44	–0.5	0.36	0.08
5780	4.44	–1.0	0.48	0.11
5780	4.44	–1.5	0.43	
5780	4.44	–2.0	0.38	
5780	4.44	–3.0	0.56	
6500	4.00	–0.0	0.12	0.05
6500	4.00	–1.0	0.78	0.33
6500	4.00	–2.0	0.60	
6500	4.00	–3.0	0.65	

now dominates the populations at least in higher atmospheric layers. The overpopulation there is enhanced and shifted further outside as compared with the solar populations because the reduced temperature decreases the kinetic energy of the particles and thus the efficiency of collisions is reduced, too.

Vice versa, quite a different population pattern is found for a 200 K hotter atmosphere. Increasing the temperature results in a significant underpopulation of the ground state; the other levels have lost their overpopulation as the line transition rates can no longer compete with the photoionization. This amounts also to a substantial overionization even in deep atmospheric layers. In this case the resonance line would be expected to show some NLTE effect which is more pronounced than for other lines.

The bottom panels in Fig. 2 imply that a variation of the stellar surface gravity has only marginal effects on the level populations (and therefore the Al I line spectrum) as long as the effective temperature is not exceeding that of the Sun. The reason is that the change of number densities of the colliding particles can not compete with the stronger radiative influence. Consequently, the variation of gravity results in NLTE effects in the line shapes almost exactly the same as those found for solar parameters under the assumption of LTE.

The discussion in the previous subsection suggests that the *metal abundance* is the parameter with the strongest influence on the statistical equilibrium. In fact, reduction of the background opacity such as encountered with decreasing metal content of the atmosphere leads to an underpopulation of all levels (Fig. 3). At solar atmospheric densities the level populations are still coupled: the underpopulation of the ground state is followed by the next higher levels and the relative overpopulation of $4s\,^2$S and $3d\,^2$D 'pulls' up the $3p\,^2$P$^{\rm o}$ population. This is no longer valid for the reduced electron densities in metal-poor stars. In the metallicity range between [Fe/H] = -1 and -2.0 the principal shape of the departure coefficients is quite similar showing a hump in the ground state population near log $\tau_{\rm c}$ = -2.5. This substantial relative increase of the lower level populations is a result of strong radiation losses in the IR lines connecting $4s\,^2$S , $3d\,^2$D and $4p\,^2$P$^{\rm o}$ with higher levels. In more metal-poor stars the lines become weaker, their formation moves inwards, and the levels $4s\,^2$S , $3d\,^2$D and $4p\,^2$P$^{\rm o}$ begin to show stronger underpopulation even in deeper layers; finally, at [Fe/H] = -3 the effect has disappeared. It is important to note that, even for [Fe/H] = -0.5, the population densities of $3p\,^2$P$^{\rm o}$ and $4s\,^2$S are no longer coupled in the photosphere since the electron collisions are too weak to thermalize the level populations. Most interestingly, this should be clearly detectable in the *wings* of the Al I resonance lines.

To gather experience with model sensitivities the combined influence of temperature, gravity, and metal abundance is demonstrated in Fig. 4, where the atomic model with a slightly different scaling factor $S_{\rm H}$ = 0.2 has been used. Again, all metal-poor atmospheres (displayed in the middle and right columns) show strong changes of the ground state populations that should be detectable in the Al I resonance lines; we note that a star such as Procyon produces similar deviations from LTE as does a metal-poor star with $T_{\rm eff}$ = 5500 K on the subgiant branch.

2.3. Line formation and abundance variations

Following the above discussion the general question arises: how do the *line profiles* vary with reduced metal content? In Fig. 5 synthetic core profiles of the resonance line at 3961 Å are compared for different metallicities with LTE profiles dashed and NLTE profiles dotted. As seen in Fig. 3 the departure coefficients

of the levels connected by the resonance line are diverging more and more as the ground state ionization increases with reduced background opacity; for the most metal-poor model, however, they seem to approach again. Except for this model all NLTE *line cores* are deeper than those calculated under LTE, due to the relative overpopulation of the $3p\,^2\mathrm{P^o}$ ground state with respect to the upper $4s\,^2\mathrm{S}$ level in the outer atmosphere. The depth of core formation which reaches chromospheric heights ($\log \tau_c \approx -6$) in solar-type stars, is shifted to -4 in the metal-poor stars, a region where the level populations are more tightly coupled. The line *core* does not depend strongly on the atmospheric structure at these depths; since the dominant radiation field is fully decoupled from the local kinetic temperature, even chromospheric temperature rises will not affect the core profile very much.

In a depth region where the *line wings* are formed the ground state is increasingly underpopulated when the metallicity is reduced. Therefore the NLTE line wings are significantly weaker than their LTE counterparts. The different shapes of the resonance line wings should affect the abundance determination. Table 1 lists the abundance corrections necessary to be applied to the LTE line formation in order to match the equivalent widths. Starting from the solar abundance towards lower metallicity the NLTE abundance effect resulting from the resonance line wings increases reaching local maxima near [Fe/H] = -1 and -3. It is largest for models with low gravity and high temperature. The NLTE abundance effect found in the excited lines (represented here by the 6696/6698 Å doublet) is smaller than in the resonance lines but is increasing with decreasing metal abundance, too. Most interestingly it is highest in models with low gravity. The different NLTE abundance *corrections* required for resonance and subordinate lines qualitatively reflect some of the systematic differences found in previous LTE abundance analyses. They also give a hint as to how the problem with the hydrogen collision rates must be solved.

It is necessary to remember the strong variation of the Al I resonance line profiles with both $T_{\rm eff}$ and $\log g$ already under the assumption of LTE. The corresponding NLTE variations are as strong or even stronger. Thus differences in equivalent width between observed and calculated profiles may be as much a result of metal abundance as of temperature or gravity.

3. Hydrogen collisions and the atomic model

It was mentioned in the previous section that the most uncertain part of the Al I atomic model refers to the representation of collisional interactions with neutral hydrogen atoms, since in metal-poor atmospheres such collision rates do not decrease (as do the rates for electron collisions). The treatment of atom-atom collisions is based on Drawin's (1968, 1969) formula which originally was derived for collisions between equal atoms. Since this approximation cannot be judged adequately from a theoretical base, different authors have introduced scaling factors $S_{\rm H}$ to estimate the importance of hydrogen collisions (cf. Lambert 1993; Takeda 1994a,b, 1995; Holweger 1995). Such a procedure must take account of every line profile observed in solar or stellar spectra.

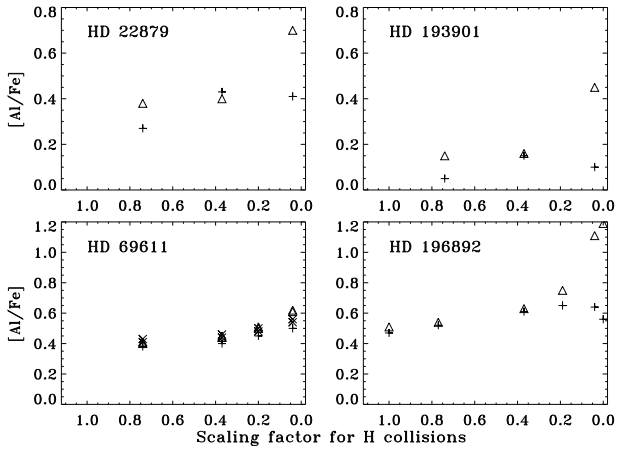

Fig. 6. Aluminium abundances obtained from line formation of different multiplets as a function of scaling factor $S_{\rm H}$. Symbols refer to 3961 Å (+), 6696 and 6698 Å (△), 8773 and 8774 Å (×)

In the Sun only a few lines in the infrared are sensitive to NLTE effects and, as outlined in Paper I, the determination of the scaling factor for hydrogen collisions is based on the synthesis of two weak *emission* features near 12 μm. On this evidence alone we arrived at a value of $S_{\rm H} = 0.002$, with none of the other solar Al lines being sensitive to hydrogen collisions at all. According to the calculations presented in the last section, in metal-poor stars NLTE effects are detectable in other lines, too, and a scaling factor $S_{\rm H} = 0.002$ applied to *all* transitions cannot produce consistent abundances for the different lines. Actually, for interactions between the lower levels a much higher value is required. A model with $S_{\rm H} = 0.4$ for these transitions finally leads to consistent abundances for all lines in all stars observed.

This is demonstrated in Fig. 6 where for a number of selected stars the NLTE Al abundances derived from different lines are plotted against the scaling parameter $S_{\rm H}$. Whereas the stellar parameters are given in Table 2 below and other details about these spectra are given in the next section, here we discuss only the determination of $S_{\rm H}$. The principal result is that without any hydrogen collisions ($S_{\rm H} = 0$) the abundances from different multiplets diverge with abundance differences being as large as 0.6 dex. For increasing $S_{\rm H} > 0$ the 6696 and 6698 Å abundances show a strong decline until $S_{\rm H} \approx 0.2$, and a nearly constant abundance level of all three multiplets for $S_{\rm H} > 0.4$ that converges towards the LTE abundance for sufficiently high values of $S_{\rm H} \gg 1$. For all stars the abundances for different lines coincide precisely only for $S_{\rm H} = 0.4$. In case of the two stars in the bottom panels the choice of $S_{\rm H}$ is not as unique, although for HD 196892 a value below 0.2 becomes unlikely. Unfortunately, for only a few stars spectra with at least two doublets were available, but in spite of the low statistical significance Fig. 6 reveals that hydrogen collisions cannot be neglected completely.

It is then possible to conclude from Fig. 6, that the atomic model adjusted to fit the solar spectrum cannot be used for metal-poor stars. A model that fits the spectra of all types of stars requires a scaling factor varying as a function of the excitation

Table 2. Stellar parameters of metal-poor stars analyzed with LTE and NLTE line formation. Data are taken from Axer et al. (A,1994) and Fuhrmann et al. (1997). [Mg/H] data are from Fuhrmann et al. (1995). Equivalent widths for λ 8772 and 8773 Å are from Edvardsson et al. (1993)

Object	$T_{\rm eff}$	log g	[Fe/H]	[Mg/Fe]	ξ	Source	[Al/Fe] abundance ratios					
	[K]				[km s^{-1}]		3961 Å		6696,6698 Å		8772,8773 Å	
							LTE	NLTE	LTE	NLTE	LTE	NLTE
HD 6434	5671	4.08	–0.68	0.34	1.26	A					0.31	0.40
HD 6582	5282	4.18	–0.94	0.30	0.75	F	0.30	0.55				
HD 19445	6040	4.52	–1.87	0.34	1.13	A	–0.50	0.10				
HD 20807	5640	3.94	–0.07	–0.08	0.57	A			–0.10	–0.10	–0.10	–0.08
HD 22879	5789	3.93	–0.85	0.39	1.35	A	–0.15	0.43	0.18	0.40		
G84-29	6364	3.72	–2.36		2.05	A	–0.50	0.10				
HD 45282	5270	3.17	–1.48	0.10	1.55	F	–0.50	0.05				
HD 51929	5606	3.53	–0.46	0.10	0.71	A					0.01	0.12
HD 69611	5593	3.58	–0.68	0.35	1.51	A	–0.10	0.40			0.37	0.46
HD 74000	6211	3.92	–1.93	0.34	1.85	F	–0.55	0.05				
G48-29	6435	4.07	–2.51	0.24	1.56	A	–0.73	–0.06				
HD 106516	5995	3.97	–0.86	0.39	1.67	A					0.22	0.37
HD 114762	5764	3.81	–0.73	0.21	1.67	A	–0.20	0.24			0.10	0.21
G64-12	6356	4.21	–3.03		1.37	A	–0.60	0.05				
HD 140283	5806	3.19	–2.48	0.22	1.55	F	–0.35	0.30				
HD 148211	5577	3.65	–0.71	0.21	1.58	A	0.13	0.24				
HD 165908	5868	4.09	–0.62	0.08	1.90	A					0.08	0.18
HD 193901	5700	4.03	–0.98		1.63	A	–0.12	0.15	0.01	0.16		
HD 194598	6040	4.30	–1.16	0.28	1.34	F	–0.50	0.05				
HD 196892	5763	3.68	–1.11		1.95	A	–0.15	0.65	0.35	0.60		
G212-7	5560	4.77	–1.60	0.09	1.91	A	–0.50	–0.20				
HD 199288	5650	3.91	–0.66	0.31	1.32	A			0.23	0.51		
HD 201891	5890	4.15	–1.11	0.20	1.24	F	–0.32	0.40				
HD 203608	5954	3.81	–0.60	0.11	1.05	A					–0.11	–0.08
G25-29	5760	3.95	–0.72		1.15	F	–0.15	0.40	0.31	0.46		
HD 205582	5630	3.08	–0.18	0.05	0.44	A	–0.30	–0.20	–0.30	–0.20		
HD 207978	6054	3.67	–0.53	0.00	1.82	A					–0.07	–0.05
HD 211998	5338	3.26	–1.40	0.34	1.30	F	–0.20	0.25				
HD 298986	6215	4.16	–1.27	0.23	1.48	A	–0.60	–0.12				

energy. Tests with $S_{\rm H}$ varying exponentially from 0.2 at 0 eV to 0.002 near 5 eV did not produce good fits. Thus we use a simple step function where $S_{\rm H}$ = 0.4 for $n_u \leq 6$ and 0.002 otherwise. These values lead to a final atomic model that is able to reproduce both the solar infrared Al I emission features and also results in abundance determinations for stars more metal-poor than the Sun that do not depend on the multiplet. Such a scaling factor cannot be put on a sound physical base, but since the abundances obtained from different lines do not vary too much with $S_{\rm H} \geq 0.5$ this semi-empirical approach must be considered satisfactory. Thus abundance errors due to NLTE modelling alone should be less than 0.1 dex.

4. Aluminium abundances in metal-poor stars

Fig. 1 displays a compilation of aluminium abundances in metal-poor stars, all obtained from LTE analyses and published as [Al/Fe] ratios. The most comprehensive is the study of Edvardsson et al. (1993) for more than 150 mildly metal-poor stars with $-1.0 \leq$ [Fe/H] $\leq +0.3$. Their results show a marginal overabundance of [Al/Fe] which tends to increase with decreasing metal abundance. Their analyses stop near [Fe/H] = -1 since they used the doublet at 8773 Å which is no longer observed for more metal-poor stars.

The results of Peterson (1981), Bessell & Norris (1984), Luck & Bond (1985), François (1986, 1988), Magain (1987, 1989), Gratton & Sneden (1987, 1988), Hartmann & Gehren (1988), Ryan et al. (1991, 1997) and McWilliam et al. (1995) add more metal-poor stars including the extreme giant CD$-38°245$ with [Fe/H] ≈ -4. In contrast to the results of the Edvardsson et al. work the LTE aluminium abundances in (extremely) metal-poor stars reveal quite a large scatter; yet a trend is detectable: nearly all stars with [Fe/H] < -1.5 are underabundant in [Al/Fe], and this underabundance is increasing with decreasing metallicity. The same results when plotted as [Al/Mg] show a more continuous decrease from solar values down to [Al/Mg] ≈ -1.5 near [Mg/H] = -2. The step-like behaviour of [Al/Fe] between [Fe/H] ≈ -1.0 and -1.5 could be a consequence of the different lines used for the investigations, since Edvardsson et al. have used the 8773 Å line whereas the other authors analyzed one or both resonance lines.

4.1. NLTE abundance analyses

A subsample of 22 stars analyzed by Axer et al. (1994) or, more recently, by Fuhrmann et al. (1997) included spectral windows with the Al I resonance lines or the 6696/6698 Å doublet and thus made possible the determination of aluminium abundances. The stellar spectra of the resonance lines were taken with the Coudé spectrograph at the Calar Alto 2.2m telescope. Line data at 6697 Å of stars in the southern hemisphere is from the Coudé Echelle Spectrograph mounted at the ESO 1.4m telescope, for northern hemisphere stars the spectra have been taken with the new FOCES Echelle Spectrograph at the Calar Alto 2.2m telescope. To these we added all stars that are in common with the analysis of Axer et al. and for which the lines at 8773 Å were available as equivalent width data from Edvardsson et al. (1993). We note that only a small number of stars have Al lines in more than one spectral window; therefore our present investigation is mostly explorative. Stellar parameters are listed in Table 2.

Synthetic spectra using either LTE or NLTE level populations were calculated using the line data given in Paper I. The line profiles were convolved with a Gaussian of appropriate width adjusted by comparison with other lines in the spectrum. Synthesis of the resonance lines included blend calculations with the Ca II H and K lines, Hε, and a number of other lines in the immediate vicinity. As discussed in Sect. 2 synthesis of the resonance lines is complicated by the problem of finding the proper continuum in the Ca II H and K window, due to the crowding of many other metal and molecular lines, a significant number of lines not even being identified. Additionally, the spectrograph cameras were all red-sensitive, and the signal in the near UV was correspondingly poor as compared with the red. Thus we cannot fully rule out *systematic* errors in determining Al abundances from the resonance lines. If these were due to line crowding, the Al abundances derived here would tend to be too low. Table 2 gives the results of the abundance analyses. The abundance errors as judged from profile syntheses with different abundances ranges from ± 0.05 to ± 0.20 dex for the resonance line, and from 0.05 to 0.10 for the 6697 Å doublet. Since only equivalent widths were used for the 8873 Å doublet, no error estimates are given here. There is no direct evidence of *systematic* errors affecting the abundances of e.g. the resonance lines in Table 2.

Results from the test calculations presented in Table 1 already show a much more pronounced NLTE effect for the resonance line than for the excited lines. Thus corrections applied to LTE analyses would be particularly large for metal-poor stars with [Fe/H] < -1 where only resonance lines determine the abundances, and they would be substantially smaller although still significant for stars of intermediate metallicity such as observed by Edvardsson et al. (1993). The step found in the LTE abundances near [Fe/H] $= -1$ (it is found as well in our own LTE data) is therefore partly removed in the NLTE results.

The strong NLTE abundance corrections with respect to LTE seem to change the present Al abundances in cool metal-poor stars completely. Among the most important results as displayed in Fig. 7 we note only three,

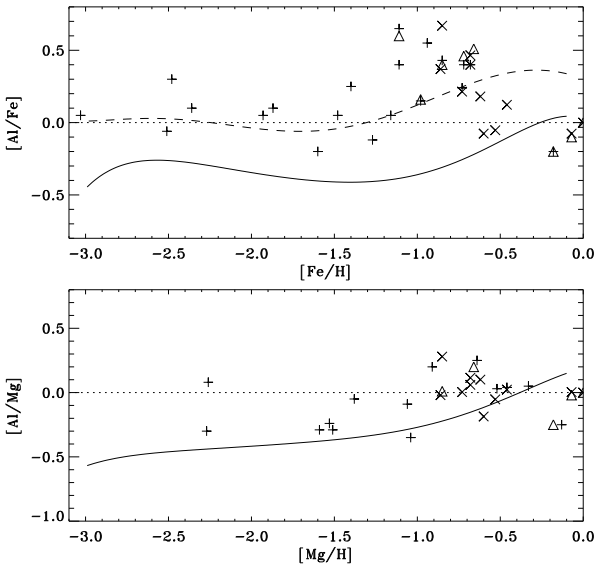

Fig. 7. [Al/Fe] and [Al/Mg] ratios obtained by fitting NLTE Al I line profile syntheses to observed spectra of metal-poor stars (cf. Table 2). These data are to be compared with the LTE results in Fig. 1. The curves represent the chemical evolution models calculated by Timmes et al. (1995). Symbols refer again to 3961 Å(+), 6696 and 6698 Å(△), 8773 and 8774 Å(×)

- The abundance scatter that is obtained for LTE analyses and evident in Fig. 1 is reduced; however, part of that could be ascribed to the small sample in our present investigation.
- Quite unexpectedly, the abundance hump obtained from LTE analyses near [Fe/H] $= -1$ has *increased* for NLTE abundances to a value of [Al/Fe] $\approx +0.5$. Among the objects defining this attribute are the bright stars HD 22879 and HD 196892, with similar abundance results from both the resonance line and the 6697 Å doublet. Therefore the Al abundances seem to be more reliable than for most of the other stars.
- For more metal-poor stars near [Fe/H] $= -1$ the overabundance disappears. Even the most extreme metal-poor stars such as G64-12 show a solar [Al/Fe] ratio, and the substantial underabundances usually found in LTE analyses are no longer found. The fact that now Al varies in lockstep with Fe is perhaps the most important result.

If instead of [Al/Fe] the [Al/Mg] ratio is plotted as a function of [Fe/H] a weak but constant underabundance of Al is found with respect to Mg, i.e. [Al/Mg] ≈ -0.2 in the most metal-poor stars. The Mg abundances used here are based on LTE results derived by Fuhrmann et al. (1995). This leads immediately to the question whether the present LTE results for the *reference elements* Fe and Mg are valid. Mg I has a strong photoionization edge at 2500 Å similar to Al I, and NLTE effects in this atom would not be surprising as was found in recent work of Zhao (1995). If in metal-poor stars the NLTE [Mg/Fe] ratio turned out to be near +0.2 instead of +0.4 (the value found from LTE analyses), [Al/Mg] = 0 would result for [Fe/H] < -1. On the other

hand, *higher* NLTE Mg abundances in extremely metal-poor stars could lead to a better fit between observations and chemical evolution calculations as shown in Fig. 7. Fe I has a similar ionization energy but its photoionization may not be as dominant as in Mg or Al. However, work in progress by Fuhrmann et al. (1997) reveals that the Fe II/Fe I ionization equilibrium is *not* following the Saha equation in stars such as HD 19445, HD 140283 or even Procyon. An investigation of the statistical equilibrium of iron is currently extended to metal-poor stars; it could perhaps lead to a better understanding of the [Al/Fe] hump near [Fe/H] = −1.

4.2. Constraints for galactic nucleosynthesis

The main production site of ^{27}Al is *hydrostatic* carbon and neon burning in SN II; contributions from explosive processes are expected to be small (Woosley & Weaver 1995). According to Nomoto et al. (1984) SN Ia do not produce significant amounts of aluminium. Consequently, the chemical evolution of aluminium in the Galaxy during the formation of the halo (and possibly a thick disk) should be tied to SN II, perhaps with a small correction for processes during H and He shell burning phases. Chemical evolution calculations based on such considerations have recently been published by Timmes et al. (1995); they are compared with the NLTE abundances in Fig. 7. The results are shown as continuous and dashed lines in Figs. 1 and 7. The dashed line refers to calculations with an iron yield decreased by a factor of two.

The discrepancy between the observed abundance ratios and chemical evolution calculations is most obvious for the LTE results, and there is apparently no way to fit the LTE observations with present knowledge about nucleosynthesis. The NLTE abundance results in Fig. 7 are so much different from their LTE counterparts that the Timmes et al. chemical evolution calculations now are in much better agreement with the observed data. However, the reduced scatter in the NLTE data makes the diffences clearly stand out from the plot. Especially for the more metal-rich objects the observed data is not compatible with the evolution curve. The hump observed in the ratio of [Al/Fe] at [Fe/H] ≈ −1 cannot be reproduced by the Timmes et al. models. For stars of lower metallicity the calculated models appear to be shifted by [Al/X] ≈ −0.3 . . . − 0.5 to lower values, where X would replace either Fe or Mg. One of the less well-known quantities in stellar nucleosynthesis is the SN II yield of Fe. The corresponding uncertainty could reach a factor of two, in which case at least the [Al/Fe] ratio for metal-poor stars would be in perfect agreement with the observations. If the hump in [Al/X] turned out to be real (and not only an artefact of spectrum analysis) any simple scenario of Galactic chemical evolution would become obsolete. It appears possible that at the time this hump was formed some additional production process became active. Calculations of Langer et al. (1993) show the possibility of additional aluminium production through mixing processes in yellow giants. Aluminium thus can be produced as a secondary element by proton capture on ^{26}Mg. This process requires mixing of Mg in regions below the oxygen shell. Due to Timmes et al. such additional production site could remove some of the discrepancies around [Fe/H] = −1, but it may not be sufficient to explain the increase in [Al/Fe]. The alternative solution for such a discontinuous change of abundance ratios then could be produced by strong variations of the *stellar mass function*.

The [Al/Mg] abundance ratio in Fig. 7 fits better to the chemical evolution calculations. A small abundance peak around [Fe/H] = −1 still seems to be present and cannot be reproduced by the calculations. It has to await further results for Mg I NLTE line formation (Zhao 1995). The nearly constant ratio found in very metal-poor stars is in marginal agreement with the evolution models, although the latter are found at an offset of $\Delta[\mathrm{Al/Mg}] \approx -0.3$. The small number of observed stars in the metal-poor region does not warrant a more detailed comparison with the results of Timmes et al.

5. Conclusions

Deviations from LTE dominate the statistical equilibrium of aluminium in metal-poor stars in such a way that Al abundances determined under the assumption of LTE are useless. NLTE line formation in particular makes it possible to obtain similar abundance results from lines of very different excitation energies. Based on the analyses of a small number of metal-poor stars it is easy to demonstrate that the previous discrepancy between LTE aluminium abundances and chemical evolution predicted with due consideration of Galactic nucleosynthesis is mostly removed when LTE abundances are replaced by the NLTE data.

In the most metal-poor stars [Al/Fe] remains at a constant value indicating that aluminium is produced mainly in a primary process. Near [Fe/H] = −1 both [Al/Fe] and [Al/Mg] display an abundance hump that is not explained with current input in Galactic chemical evolution calculations. This must not necessarily be causally connected with Galactic disk formation; it could as well be due to badly understood NLTE formation of Mg and Fe lines. Besides some smaller problems this hump is the present challenge to either stellar spectroscopic methods or stellar nucleosynthesis theory. A second contradictory trend that remains to be solved is the *decrease* of [Al/Fe] with increasing [Fe/H] as found in both LTE and NLTE analyses of stars more metal-rich than [Fe/H] = −1. Such a trend is at variance with chemical evolution which requires an *increase* of [Al/Fe] towards solar metal abundance.

In the light of the present results for aluminium it may be unavoidable to reinvestigate the spectrum analysis of other elements such as magnesium and iron. Most of our knowledge about the evolution of the Galaxy is based on one of these two elements, and much of if may be obsolete in view of substantial NLTE effects that are possible in metal-poor stars.

Acknowledgements. This research was supported by the Deutsche Forschungsgemeinschaft under grant Ge 490/10-1 and -2. We thank K. Butler for his strong support with atomic data and for continuous help with the line formation code, and J. Reetz for many discussions.

References

Arpigny, C., Magain, P. 1983, A&A 127, L7
Axer, M., Fuhrmann, K.,Gehren, T. 1994, A&A 291, 895
Baumüller, D., Gehren, T. 1996, A&A, 307, 961 (Paper I)
Bessell, M.S., Norris, J. 1984, ApJ 285, 622
Böhm-Vitense, E. 1958, Z. Astrophys. 46, 108
Bruls, J.H.M.J., Rutten, R.J., Shchukina, N.G. 1992, A&A 265, 237
Butler, K., Giddings, J. 1985, Newsletter on the Analysis of Astronomical Spectra No. 9, University of London
Drawin, H.W. 1968, Z. Physik 211, 404
Drawin, H.W. 1969, Z. Physik 225, 470
Edvardsson, B., Anderson,J., Gustafsson, B. et al., 1993, A&A 275,101
François, P. 1986, A&A 160, 264
François, P. 1988, A&A 195, 226
Fuhrmann, K., Axer, M., Gehren, T. 1993, A&A 271, 451
Fuhrmann, K., Axer, M., Gehren, T. 1995, A&A 301, 492
Fuhrmann, K., Pfeiffer, M., Frank, C., Reetz, J., Gehren, T. 1997, A&A in press
Gehren, T. 1977, A&A 59, 303
Gratton, R.G., Sneden, C. 1987, A&A 178, 179
Gratton, R.G., Sneden, C. 1988, A&A 204, 193
Hartmann, K., Gehren, T. 1988, A&A 199, 269
Holweger, H., 1995, Phys. Scripta, in press
Kurucz, R.L. 1992, Rev. Mex. Astron. Astrof. 23, 181
Lambert, D.L. 1993, Phys. Scripta T47, 186
Langer, G.E., Hoffman, R., Sneden, C. 1993, PASP 105, 301
Luck, R.E., Bond, H.E. 1985, ApJ 292, 559
Magain, P. 1987, A&A 179, 176
Magain, P. 1989, A&A 209, 211
McWilliam, A., Preston, G., Sneden, C., Searle, L. 1995, AJ 109, 2757
Nomoto, K., Thielemann, F.K., Yokoi, K. 1984, ApJ 286, 644
Peterson, R.C. 1981, ApJ 244, 989
Regemorter, H. van 1962, ApJ 136, 906
Ryan, S.G., Norris, J.N., Bessel, M.S. 1991, AJ 102,303
Ryan, S.G., Norris, J.N., Beers, T.C. 1997, ApJ in press
Steenbock, W., Holweger, H. 1984, A&A 130, 319
Takeda. Y. 1994a, PASJ 46, 53
Takeda. Y. 1994b, PASJ 46, 395
Takeda. Y. 1995, PASJ 47, 463
Thielemann, F.K., Nomoto, K., Yokoi, K. 1986, A&A 158, 17
Timmes, F.X., Woosley, S.E.,Weaver, T.A. 1995, ApJS 98, 617
Vitense, E. 1953, Z. Astrophys. 32, 135
Woosley, S.E., Waever. T.A. 1986, ARAA 24, 205
Woosley, S.E., Waever. T.A. 1995, ApJS 101, 181
Zhao, G. 1995, private communication

This article was processed by the author using Springer-Verlag LaTeX A&A style file *L-AA* version 3.